doi.org/10.36721/PJPS.2026.39.3.REG.14944.1

Mechanism of Keap1-Nrf2-HO-1/GPX4 signal in blocking epileptic hippocampal neuron ferroptosis and intervention effect of Caogouzhimu decoction

Dandan Zhang*, Zhimin Yu and Jun Zhang
Department of Neurology I, Jingmen People's Hospital, Hubei, China

Abstract: **Background**: The pathogenesis of epilepsy is closely associated with ferroptosis in hippocampal neurons. The Keap1-Nrf2-HO-1/GPX4 signaling pathway serves as a crucial endogenous antioxidant system and plays a significant role in regulating cellular ferroptosis. Caogouzhimu decoction has demonstrated potential antiepileptic effects in clinical practice, yet whether it intervenes in neuronal ferroptosis via this signaling pathway remains unclear. **Objective**: To explore the mechanism of the Keap1-Nrf2-HO-1/GPX4 signaling pathway in ferroptosis of hippocampal neurons in epilepsy and evaluate the intervention effect of Caogouzhimudecoction. **Methods**: Fifty mice were divided into a blank control group, a model control group and low-, medium- and high-dose Caogouzhimu decoction groups, with ten mice per group. The epilepsy model was induced by PTZ and the treatment groups received intragastric administration of Caogouzhimu decoction at doses of 40, 80 and 120 mg/mL, respectively. Behavior, hippocampal dentate gyrus neurogenesis and the expression levels of components related to the Keap1-Nrf2-HO-1/GPX4 signaling pathway were compared among the groups. **Results**: The high-dose group exhibited significantly shorter latency, reduced swimming distance and fewer convulsions above grade II compared to the other groups ($P<0.05$). Furthermore, the high-dose treatment effectively suppressed neurogenesis in the hippocampal dentate gyrus and the occurrence of ferroptosis, as evidenced by significantly lower mRNA expression levels of Keap1, Nrf2, HO-1 and GPX4 compared to those in the low- and medium-dose groups ($P<0.05$). **Conclusion**: Caogouzhimu decoction exerts anti-epileptic effects, likely by inhibiting hippocampal neuronal ferroptosis through modulation of the Keap1-Nrf2-HO-1/GPX4 signaling pathway. These findings provide a novel perspective for the clinical treatment of epilepsy.

Keywords: Caogouzhimu decoction; Epilepsy; Ferroptosis; Hippocampal neurons; Intervention mechanism; Keap1-Nrf2-HO-1/GPX4 signal

Submitted on 31-07-2025 – Revised on 13-11-2025 – Accepted on 09-12-2025

INTRODUCTION

Epilepsy is characterized by sudden abnormal discharges of brain neurons (Feng *et al*., 2024). According to epidemiological data, the prevalence of epilepsy in China is approximately 7 per 1,000 individuals, with an annual incidence of 28.8 per 100,000 population and a one-year active epilepsy incidence of 4.6% (Nandan *et al*., 2023). Consequently, it is estimated that China has approximately 9 million individuals with epilepsy, of whom 5-6 million are affected by active epilepsy. Its prevalence is increasing at a relatively rapid rate, significantly affecting patients' health and lives. The etiology of epilepsy is complicated and it is generally considered to be related to genetic factors, brain diseases, or systemic conditions. Clinical manifestations are mostly seizures, tonic seizures, spasms, etc (Liao *et al*., 2025). The Keap1-Nrf2-HO-1/GPX4 signaling pathway serves as a vital endogenous antioxidant system, playing a crucial role in maintaining oxidative homeostasis. Nuclear factor erythroid 2-related factor 2 (Nrf2) is an important endogenous antioxidant transcription factor in brain tissue and is often regulated by Kelch-ECH-related keap1 (Kaur *et al*., 2021). Under normal physiological conditions, Keap1 protein and Nrf2 can bind to each other in the cell, leading to its ubiquitination and degradation, thereby maintaining low expression levels in a dynamic balance. However, when a large amount of ROS is produced in the body, Keap1 is subject to oxidative damage. The reactive oxygen species (ROS) can cause the conformational abnormality of Keap1, thereby releasing Nrf2 and increasing the expression of phase II detoxifying enzymes and antioxidant proteases (Li *et al*., 2021). Previous research indicates that Nrf2 overactivation can alleviate brain damage and ameliorate epileptic symptoms (Xie *et al.,* 2022); however, the underlying mechanisms remain incompletely understood. Caogouzhimu decoction, a traditional Chinese medicinal formula, is known for its effects in clearing irritability, moistening dryness, nourishing yin, and clearing heat. Nevertheless, its potential role in epilepsy has been scarcely explored (Tao *et al*., 2023). Therefore, this study aimed to explore the mechanism of Keap1-Nrf2-HO-1/GPX4 signaling pathway in blocking hippocampal neuronal ferroptosis in epilepsy and the interventional effect of Caogouzhimu decoction.

**Corresponding author:* e-mail: yeshangqie2@163.com

MATERIALS AND METHODS

Clinical data

A total of fifty young mice were acquired between June 2018 and January 2019. Ten mice were randomly assigned as the blank control group, while the remaining forty were utilized to establish a PTZ-induced epilepsy model. Ten mice were randomly selected as the model control group. The remaining 30 mice were administered Caogouzhimu decoction at three different doses: low-dose (40 mg/mL), medium-dose (80 mg/mL) and high-dose (120 mg/mL), with 10 mice in each group. The dose selection was based on previous pharmacological studies demonstrating the efficacy and safety of Caogouzhimu decoction in similar experimental models. All mice, obtained from Laboratory Animal Co., Ltd., had a weight range of 19-21 g, with an average of 20.59±0.76 g. The animal license number was SCXK (Shanghai) 2017-0005. Mice were routinely fed for one week prior to the experiment and housed in cages at 20-24^{o}C with a humidity of 40%-60%.

Instruments

Instrument list as listed in Table 1.

Methods

(1) *Preparation and quality control of Caogouzhimu decoction*: Caogouzhimu decoction was composed of 12 g of Caoguo (Amomum tsaoko) and 12 g of Zhimu (Anemarrhena asphodeloides) in dry weight. The herbs were soaked in ten volumes (v/w) of distilled water for 30 minutes, followed by two rounds of reflux extraction, each lasting 1.5 hours. The combined extracts were filtered and the filtrate was concentrated to a final concentration of 1 g/mL (crude drug) using a rotary evaporator. The concentrate was aliquoted and stored at 4^{o}C for use within one week. To ensure batch-to-batch consistency, high-performance liquid chromatography (HPLC) was employed to quantitatively analyze the characteristic active components, such as sarsasapogenin in Zhimu.

(2) *Modeling method*: Fifty young mice were purchased as subjects and 10 were randomly selected as blank control groups; the remaining 40 mice were induced by PTZ to establish an animal model of epilepsy. Refer to relevant literature to complete the preparation of PTZ solution (concentration 10 mg/mL). The mice received daily intraperitoneal injections of PTZ solution (0.03 mL/kg) for 28 consecutive days. After a one-week drug withdrawal period, seizure behaviors were assessed according to the Racine scoring method. The model was considered successful if more than five convulsions of class II – IV were observed per week during the post-withdrawal period (Mao *et al*., 2024).

(3) *Treatment method*: Fifty young mice were randomly divided into five groups (n=10): blank control group (normal feeding), model control group (PTZ-induced model + equal volume of physiological saline) and low-, medium- and high-dose Caogouzhimu decoction groups (He *et al*.,1999; administered 40 mg/mL, 80 mg/mL and 120 mg/mL of the decoction by gavage once daily for 14 consecutive days), positive control group: (PTZ-induced epilepsy model with standard anti-epileptic drugs).

Detection method

(1) *Behaviors of mice*: The behavior of the mice was assessed using the Morris water maze 14 days after the intervention in each group. The water maze system is composed of a pool with a height of 50 cm and a diameter of 200 cm, black background and a 10cm-diameter black platform with adjustable height and movement. Pour clean water (20-22 cm depth, temperature 25^{o}C) into the system and divide it into four different spaces. During testing, mice were randomly placed into one of four starting quadrants to initiate the behavioral assessment. Latency period and path efficiency: The latency period (the duration to find the platform) and the swimming distance (the total path length traveled) were recorded respectively for each mouse (Forero *et al*., 2023).

(2) *Hippocampal dentate neurons*: After 4 days of intervention, 5 mice per group were euthanized via cervical dissection. Hippocampal tissue was collected through rapid whole-brain isolation on ice. The brain was then cut along the sagittal suture, and the hippocampus was identified and dissected based on anatomical landmarks, including the lateral ventricles and its characteristic arched structure. During paraffin sectioning, continuous coronal sections with a thickness of 5 μm were prepared. Sections within the range of approximately -1.34 mm to -2.46 mm posterior to the bregma were selected for staining to ensure the inclusion of the complete hippocampal dentate gyrus structure. The dentate gyrus was identified by its distinct C-shaped granule cell layer and the morphological characteristics of the hilus (Zhong *et al*., 2023). Immunohistochemical staining was performed to detect astrocyte pyroptosis-related markers in the dentate gyrus. Primary antibodies used included: rabbit anti-mouse GPX4 polyclonal antibody (Beijing Boao Sen, 1:200) for pyroptosis-suppressing proteins; rabbit anti-mouse ACSL4 polyclonal antibody (Beijing Boao Sen, 1:200) for pyroptosis-promoting proteins; and NeuN monoclonal antibody (1:500, Abcam) as a neuron-specific marker to confirm neuronal localization. Secondary antibody was HRP-labeled goat anti-rabbit IgG (1:5000) with DAB chromogenic reaction. Sections were observed under inverted microscopy and images captured to analyze the number of NeuN-positive neurons and the expression/distribution patterns of GPX4 and ACSL4 in the dentate gyrus region.

(3) *Keap1-Nrf2-HO-1/GPX4 signal expression*: After 4 days of intervention, 5 mice were sacrificed by cervical dislocation in each group and 5 mL of arterial blood was collected and stored. For Western blot analysis, a portion of hippocampal tissue was lysed in RIPA lysis buffer containing protease inhibitors. The separated serum sample was treated with 500μL of Trizol reagent and mixed

thoroughly. Subsequently, 1.0 mL of the mixture was transferred to a centrifuge tube, vortexed for 5 minutes, and allowed to stand. Added 200μL chloroform to the two groups of serum samples for 15secs, shook, after 5 minutes of rest, centrifuged at 12,000 × g for 15 minutes at 4°C. The supernatant was removed; 1 mL pre-cooled ethanol (concentration 75.0%) was added and dried at room temperature for 7 minutes; The absorbance was then measured using a UV spectrophotometer at 260 nm.

① *Western Blot Analysis*: For Western blot analysis, hippocampal tissues were homogenized in RIPA lysis buffer containing protease inhibitors. The protein concentration was determined using the BCA method. Protein samples were denatured by heating at 95°C for 5 minutes in loading buffer. Equal amounts of protein were separated by SDS-PAGE and transferred to PVDF membranes. After blocking with 5% skim milk, the membranes were incubated overnight at 4°C with the following primary antibodies: Keap1 (1:1000), Nrf2 (1:1000), HO-1 (1:1500), GPX4 (1:2000) and β-actin (1:5000). Commercial recombinant proteins were used as positive controls. Following incubation with HRP-conjugated secondary antibodies, the protein bands were visualized using an ECL detection system. The grayscale values of the bands were analyzed using ImageJ software and the relative expression levels of the target proteins were normalized to that of β-actin.

② *Semi-quantitative RT-PCR Analysis*: Total RNA was extracted from hippocampal tissue using the Trizol method. The concentration and purity of the RNA were quantified using a NanoDrop 2000 spectrophotometer by measuring the absorbance at 260 nm. Samples with an A260/A280 ratio between 1.8 and 2.0 were used for subsequent experiments. 1μg total RNA sample was used for cDNA synthesis via the RevertAid First Strand cDNA Synthesis Kit in a 20μL reaction system. The thermal cycling conditions were: 25°C for 5 min, 42°C for 60 min and 70°C for 5 min. Amplification was performed using SYBR Green qPCR Master Mix on a QuantStudio 5 real-time PCR instrument. The reaction system (20μL) contained: 10μL SYBR Green Mix, 0.8μL upstream primer (10μM), 0.8μL downstream primer (10μM), 2μL cDNA template and 6.4μL RNase-free water. The cycling program was: 95°C denaturation for 10 mins; followed by 40 cycles of 95°C for 15 secs and 60°C for 30 secs. The mRNA expression levels of Keap1, Nrf2, HO-1 and GPX4 were analyzed using conventional RT-PCR for semi-quantification. The PCR products were separated by 1.5% agarose gel electrophoresis, visualized and photographed using a gel imaging system. The band intensity was analyzed with ImageJ software and the relative mRNA expression levels were represented by the grayscale ratio of the target genes to the internal reference β-actin (Vo *et al*., 2025) (Table 2).

Statistical analysis

It was processed by SPSS18.0 software. The count data was detected by χ^2 test and expressed by n (%) and the measurement data adopted t-test and was expressed by $\bar{x} \pm s$. P<0.05 was statistically significant.

RESULTS

Mice behavioral comparison

Compared with the model control group, all Caogouzhimu decoction groups exhibited significantly shorter latency periods, reduced swimming distances, and fewer convulsions above grade II (all P<0.05). However, these parameters remained higher than those in the blank control group (P<0.05). Notably, the high-dose group showed significantly lower values for latency, swimming distance, and grade II convulsions compared to both the low- and medium-dose groups (P<0.05). Similarly, the medium-dose group demonstrated significant improvements over the low-dose group (P<0.05) (Table 3).

Comparison of hippocampal dentate neurons in each group

Immunohistochemical analysis revealed that the blank control group exhibited fewer NeuN-positive cells in the hippocampal dentate gyrus, with no evident dentate granule cell clusters and minimal ferroptosis. In contrast, the model control group showed clustered NeuN-positive cells and pronounced ferroptosis. Among the treatment groups, varying degrees of NeuN-positive cell clustering and ferroptosis were observed, with the high-dose group displaying the mildest ferroptotic changes (Fig. 1).

Keap1-Nrf2-HO-1/GPX4 signal comparison of each group

Semi-quantitative RT-PCR analysis indicated that the mRNA expression levels of Keap1, Nrf2, HO-1, and GPX4 in all Caogouzhimu decoction groups were significantly lower than those in the model control group P< 0.05), yet remained higher than those in the blank control group (P< 0.05). Furthermore, expression levels in the medium-dose group were significantly reduced compared to the low-dose group (P<0.05) (Table 4 and Fig. 2).

DISCUSSION

The etiology of epilepsy is complex and is generally associated with neuronal apoptosis and ion channel dysfunction. The early clinical symptoms of patients lack typicality, but with the continuous development of the disease, it will cause neurological and cognitive changes and affect the patient's health and life (Hu *et al*., 2024). In this study, a pentylenetetrazol (PTZ)-induced epilepsy model was established in mice. PTZ, a chemical convulsant, exerts its pro-epileptic effects by stimulating the central nervous system, leading to tonic-clonic seizures in rodents. Previous research has demonstrated that PTZ can induce epileptogenesis and seizures in animal models, which closely resemble human epilepsy (Singh *et al*., 2021). It lays the foundation for subsequent research.

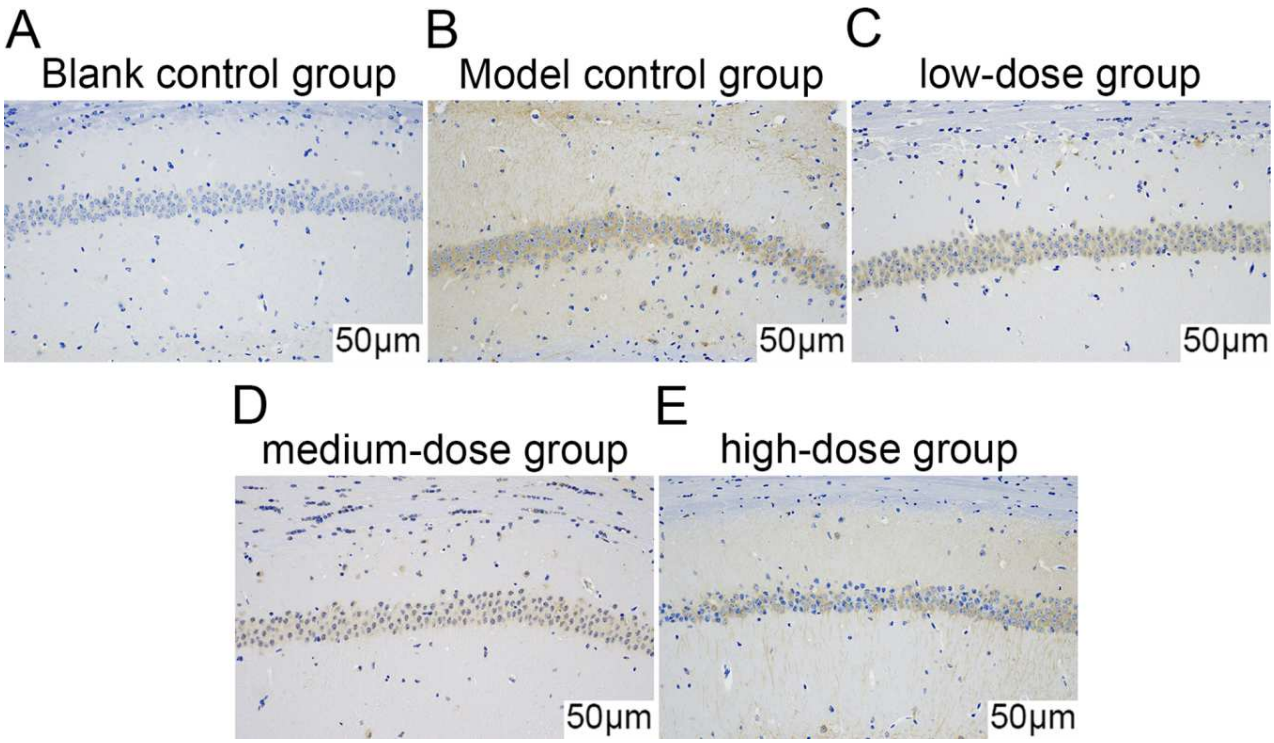

Fig. 1: Immunohistochemical staining of hippocampal dentate gyrus in each group (× 200)
Note: (A) shows the data of immunohistochemistry in the blank control group; (B) shows the data of immunohistochemistry in the model control group; (C) shows the data of low-dose immunohistochemistry; (D) shows the data of medium-dose immunohistochemistry; (E) shows the data of high-dose group Immunohistochemistry.

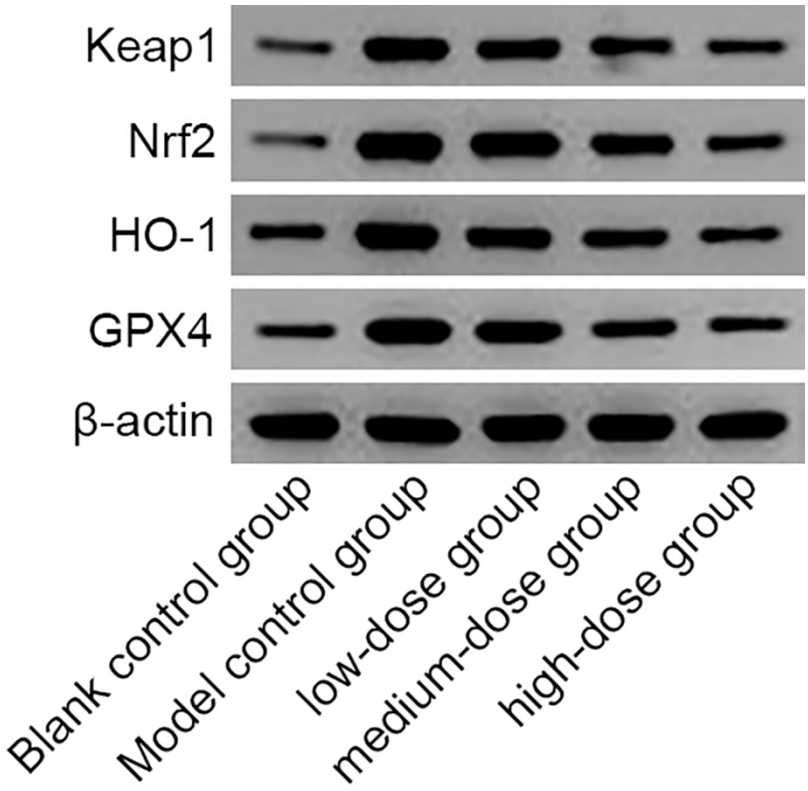

Fig. 2: Keap1-Nrf2-HO-1/GPX4 signal of each group

Table 1: Instruments

Instruments	Manufacturers
PTZ	Sigma corporation
Penicillin sodium	Yuekang Pharmaceutical Group Co., Ltd
Rabbit anti-mouse GPX4 polyclonal antibody	Beijing Boaosen Biotechnology Co., Ltd
Rabbit anti-mouse ACSL4 polyclonal antibody	Beijing Boaosen Biotechnology Co., Ltd
NeuN monoclonal antibody	Abcam, USA
RNA reverse transcription Kit	Invitrogen, USA
Trizol total RNA extraction box	Invitrogen, USA
Inverted microscope	Olympus
PCR amplifier	Xi'an Baoyude Company
Low-temperature high-speed centrifuge	Johnson & Johnson Medical Devices Co., Ltd.
PBS	Beijing Zhongshan Jinqiao Company

Table 2: Primer sequences

Premier type	Premier	Length
Keap1	F:5' CAACTTCGCTGAGCAGATTGGC 3' R:5' TGATGAGGGTCACCAGTTGGCA3'	134
Nrf2	F:5' CACATCCAGTCAAACCAGTGC3' R:5'GGAATGTCTGCGCCAAAAGCTG 3'	112
HO-1	F:5' CCAGGCAGAGAATGCTGAGTTC3' R:5' AAGACTGGGCTCTCCTTGTTGC 3'	144
GPX4	F:5' AGTGGATGAAGATCCAACCCAAGG3' R:5' GGGCCACACACTTGTGGAGCTACA 3'	180

Table 3: Behavioral comparison of mice in each group

Groups	Numbers	Latency time(s)	Swimming distance (cm)	Convulsions above level II
Low-dose group	10	30.29 ± 5.39^{abcd}	406.34 ± 22.51^{abcd}	11.49 ± 1.33^{abcd}
Medium-dose group	10	24.34 ± 4.12^{abc}	350.69 ± 18.74^{abc}	9.34 ± 1.26^{abc}
High-dose group	10	15.43 ± 4.38^{ab}	295.38 ± 15.82^{ab}	5.69 ± 1.12^{ab}
Model control group	10	43.69 ± 5.71^{a}	460.38 ± 25.68^{a}	14.79 ± 2.15^{a}
Blank control group	10	12.58±3.96	240.12±12.15	2.09±0.79

$^{a,b,c,d}P<0.05$ refer to the comparison with blank model, control model, low-dose, and medium-dose group.

Table 4: Semi-quantitative RT-PCR analysis of genes associated with the Keap1-Nrf2-HO-1/GPX4 signaling pathway in hippocampal tissue.

Group	Number	Keap1	Nrf2	HO-1	GPX4
Low-dose groups	10	0.67 ± 0.12^{abcd}	0.71 ± 0.10^{abcd}	0.75 ± 0.16^{abcd}	0.61 ± 0.12^{abcd}
Medium-dose group	10	0.58 ± 0.11^{abc}	0.59 ± 0.09^{abc}	0.68 ± 0.16^{abc}	0.46 ± 0.08^{abc}
High-dose group	10	0.41 ± 0.09^{ab}	0.36 ± 0.05^{ab}	0.58 ± 0.18^{ab}	0.39 ± 0.07^{ab}
Model control group	10	0.89 ± 0.13^{a}	0.87 ± 0.11^{a}	0.90 ± 0.14^{a}	0.86 ± 0.09^{a}
Model control group	10	0.32±0.07	0.25±0.05	0.41±0.14	0.31±0.06

$^{a,b,c,d}P<0.05$ refer to the comparison with blank model, control model, low-dose, and medium-dose group.

The Keap1-Nrf2-HO-1/GPX4 signaling pathway constitutes a critical endogenous antioxidant system, playing a pivotal role in maintaining cellular redox homeostasis (Yu and Xiao 2021). Within the brain, Nrf2 serves as a key transcriptional regulator of antioxidant responses.

Previous studies have demonstrated that Nrf2 over activation can mitigate oxidative damage following cerebral ischemic injury (Chen *et al*., 2023). It is noteworthy, however, that Nrf2 activation exhibits a dual role. In chronic neurological disorders such as epilepsy, while initial Nrf2 activation serves as an endogenous protective response to combat oxidative stress and neuroinflammation, prolonged or excessive activation may also have adverse effects. Overactive Nrf2 could disrupt normal cellular redox homeostasis, potentially hindering long-term recovery by promoting uncontrolled cell proliferation or interfering with apoptosis. Furthermore, in certain diseases, sustained Nrf2 activation is associated with chemotherapy resistance. Meanwhile, among the activated antioxidant genes, HO-1 can exert protective effects against ischemia-reperfusion injury and inhibition of HO-1 has been shown to aggravate the condition (Nguyen *et al*., 2024). This suggests that both Nrf2 and HO-1 may serve as potential therapeutic targets in the

oxidative stress processes involved in epilepsy development. Domestic research results show that (Huang *et al*., 2022) a large number of ROS over-activated autophagy and increased apoptosis play an important and versatile role in cell proliferation and growth.

Autophagy can also occur under normal physiological conditions but it can also be caused by physiological and pathological stimuli. Clinical studies have shown that (Liu *et al*., 2025). Keap1-Nrf2-HO-1/GPX4 significantly increases in multiple epilepsy sites, cause neuronal rupture and trigger chronic neuronal apoptosis, thus cause neuronal necrosis. It can be seen that Keap1-Nrf2-HO-1/GPX4 has played an important part in the treatment of epilepsy and is expected to become a new target for epilepsy.

Caogouzhimu decoction is a classical traditional Chinese medicine formula, originating from the *Jinkui Yaolue*. It is primarily composed of the herbs Caoguo (Amomum tsao-ko) and Zhimu (Anemarrhena asphodeloides). It can nourish yin and remove inner heat, thus has a nourishing effect on heart and lungs. Modern pharmacological results show that (Zhou *et al*., 2022) Zhimu has good antioxidant effect, containing salsa saponin, thus can protect the prefrontal-marginal structure of the mouse brain and can attenuate neurotrophic factor/tyrosine protein kinase gene signals in the brain. It can also block brain tissue proto-oncogene, increase neuron activity, synaptic function and plasticity and inhibit neuron damage. Studies by domestic scholars have shown that Caogouzhimu decoction can improve the behaviors of depressed mice, weaken the extracellular regulatory kinase 1/2 pathway and protect hippocampal neuron apoptosis to the greatest extent (Weijia *et al*., 2025). In the present study, the high-dose group demonstrated significantly shorter latency, reduced swimming distance, and fewer grade II or above convulsions compared to the low- and medium-dose groups ($P < 0.05$). Similarly, the medium-dose group showed significant improvements in these behavioral parameters relative to the low-dose group ($P < 0.05$). These results suggest that Caogouzhimu decoction ameliorates epilepsy-associated neurobehavioral deficits and promotes functional recovery. It has been reported that hippocampal dentate gyrus neurogenesis after epilepsy can cause neuroplasticity changes and cause the deterioration of epilepsy. Caogouzhimu decoction is reported to modulate hippocampal levels of acetylcholine (ACh), endorphins (ED), and serotonin (5-HT), among other central mediators, and to regulate the balance between excitatory and inhibitory amino acids, thereby suppressing aberrant neurogenesis in the hippocampal gyrus (Zhang *et al*., 2023). In this study, immunohistochemical results showed that there were multiple clustered hippocampal dentate neuron-positive cells in different dose groups and high-dose group. Ferroptosis in each group was of varying degrees but at a low content in the high-dose group, followed by the medium-dose group. In order to further determine the expression of this signal in epilepsy mice and the effect of Caogouzhimu decoction, the related signal was tested in this study. The results showed that GPX4 mRNA and other related signal levels in high-dose group were lower than those in other two groups ($P<0.05$); Keap1, Nrf2, HO-1 and GPX4 mRNA levels in the medium-dose group were lower than those in the low-dose group ($P<0.05$), indicating that the intervention of Caogouzhimu decoction can improve the signaling pathway in mice and the symptoms of epilepsy.

Although this study has yielded significant findings, several limitations should be noted. First, the study only focused on mRNA levels to detect changes in the Keap1-Nrf2-HO-1/GPX4 signaling pathway and did not validate these findings at the protein level using methods such as Western blotting, which limits the comprehensiveness of the conclusions regarding pathway activity. Additionally, conventional RT-PCR was used for gene expression analysis. While this method can reflect expression trends between groups, its quantitative accuracy is inferior to that of quantitative real-time PCR (qRT-PCR). Future studies should employ qRT-PCR to provide more precise quantitative data. Second, the short duration of this study precluded evaluation of the long-term therapeutic effects and potential side effects of Caogouzhimu decoction on epilepsy. Finally, the assessment of ferroptosis in this study primarily relied on morphological observations. In future work, specific biochemical assays should be incorporated for a more comprehensive analysis.

CONCLUSION

In summary, Keap1-Nrf2-HO-1/GPX4 signal can block epilepsy hippocampal neurons ferroptosis. Intervention of high-dose Caogouzhimu decoction can improve behaviors of mice and reduce the neurogenesis of hippocampal gyrus and provide new ideas and methods for epilepsy treatment.

Acknowledgment
We gratefully acknowledge Jingmen People's Hospital for providing the necessary equipment for this study.

Author's contribution
Jun Zhang analyzed the data, drafted the manuscript and was the primary contributor to writing this manuscript.
Zhimin Yu collected the data. Dandan Zhang conceived and designed the study, provided funding support and made substantial revisions and critical reviews of the article.

Funding
There was no funding.

Data availability statement
All data generated or analysed during this study are included in this published article.

Ethical approval
This study was approved by the ethics committee of Jingmen People's Hospital (No. JM20240505E).

Conflict of interest

The authors declare that the study was conducted in the absence of any commercial or financial interests that could be interpreted as a potential conflict of interest.

REFERENCES

Chen Y, He W, Wei H, Chang C, Yang L, Meng J, Long T, Xu Q and Zhang C (2023). Srs11-92, a ferrostatin-1 analog, improves oxidative stress and neuro inflammation via Nrf2 signal following cerebral ischemia/reperfusion injury. *CNS Neurosci Ther*., **29**(6): 1667–1677.

Feng F, Luo R, Mu D and Cai Q (2024). Ferroptosis and pyroptosis in epilepsy. *Mol Neurobiol*., **61**(10): 7354–7368.

Forero MG, Hernández NC, Morera CM, Aguilar LA, Aquino R and Baquedano LE (2023). A new automatic method for tracking rats in the Morris water maze. *Heliyon*., **9**(7): e18367.

He J, Liang Y and Wang H (1999). Effect of caoguo zhimu decoction on N-methyl-D-aspartate receptor gene expression of epileptic kindling model in rats. *Chin J Integr Med.*, **19**(10), 617–619.

Hu Y, Qi H, Yang J, Wang F, Peng X, Chen X and Zhu X (2024). Wogonin mitigates microglia-mediated synaptic over-pruning and cognitive impairment following epilepsy. *Phytomedicine*., **135**: 156222.

Huang Z, Gan S, Zhuang X, Chen Y, Lu L, Wang Y, Qi X, Feng Q, Huang Q, Du B, Zhang R and Liu Z (2022). Artesunate inhibits the cell growth in colorectal cancer by promoting ROS-dependent cell senescence and autophagy. *Cells*, **11**(16): 2472.

Kaur G, Sharma A and Bhatnagar A (2021). Role of oxidative stress in pathophysiology of rheumatoid arthritis: Insights into NRF2-KEAP1 signalling. *Autoimmunity*, **54**(7): 385–397.

Li J, Lu K, Sun F, Tan S, Zhang X, Sheng W, Hao W, Liu M, Lv W and Han W (2021). Panaxydol attenuates ferroptosis against LPS-induced acute lung injury in mice by Keap1-Nrf2/HO-1 pathway. *J Transl Med*., **19**(1): 96.

Liao Q, Guo Z, Ding C, Zuo R and Liu G (2025). Integrating network analysis and experimental validation to reveal the ferroptosis-associated mechanism of velvet antler in the treatment of chronic atrophic gastritis. *J Food Drug Anal*., **33**(2): 119–131.

Liu Z, Li Y, Bao J, Li S, Wen Y, Zhang P, Feng J, Wang Y, Tian L and Jie Y (2025). Astaxanthin ameliorates benzalkonium chloride-induced dry eye disease through suppressing inflammation and oxidative stress via Keap1-Nrf2/HO-1 signaling pathways. *Animal Model Exp Med*., **8**(6): 1056–1079.

Mao R, Hu M, Liu X, Ye L, Xu B, Sun M, Xu S, Shao W, Tan Y, Xu Y, Bai F and Shu S (2024). Impairments of GABAergic transmission in hippocampus mediate increased susceptibility of epilepsy in the early stage of Alzheimer's disease. *Cell Commun Signal*., **22**(1): 147.

Nandan A, Zhou YM, Demoe L, Waheed A, Jain P and Widjaja E (2023). Incidence and risk factors of post-stroke seizures and epilepsy: Systematic review and meta-analysis. *J Int Med Res*., **51**(11): 3000605231213231.

Nguyen CD, Yoo J, Jeong SJ, Ha HA, Yang JH, Lee G, Shin JC and Kim JH (2024). Melittin - the main component of bee venom: A promising therapeutic agent for neuroprotection through keap1/Nrf2/HO-1 pathway activation. *Chin Med*., **19**(1): 166.

Singh T, Mishra A and Goel RK (2021). PTZ kindling model for epileptogenesis, refractory epilepsy and associated comorbidities: Relevance and reliability. *Metab Brain Dis*., **36**(7): 1573–1590.

Tao F, Cai Y, Deng C, Chen Z, Shen Y and Sun H (2023). A narrative review on traditional Chinese medicine prescriptions and bioactive components in epilepsy treatment. *Ann Transl Med*., **11**(2): 129.

Vo K, Shila S, Sharma Y, Pei GJ, Rosales CY, Dahiya V, Fields PE and Rumi M AK (2025). Detection of mRNA transcript variants. *Genes (Basel).*, **16**(3): 343.

Weijia LI, Jing LU, Chao MA, Mengmeng L, Ke P, Hongyan C, Zhe L and Guangfu L (2025). Hamayou protein hydrolysate ameliorates depression by regulating the mitogen-activated protein kinase pathway. *J Tradit Chin Med*., **45**(3): 493–507.

Xie R, Zhao W, Lowe S, Bentley R, Hu G, Mei H, Jiang X, Sun C, Wu Y and Yueying Liu (2022). Quercetin alleviates kainic acid-induced seizure by inhibiting the Nrf2-mediated ferroptosis pathway. *Free Radic Biol Med*., **191**: 212–226.

Yu C and Xiao JH (2021). The Keap1-Nrf2 System: A Mediator between Oxidative Stress and Aging. *Oxid Med Cell Longev*, 2021.

Zhang S, Zhang Y, Zheng Y, Zhu S, Sun J, Deng Y, Wang Q and Zhai Q (2023). Dexmedetomidine attenuates sleep deprivation-induced inhibition of hippocampal neurogenesis via VEGF-VEGFR2 signaling and inhibits neuroinflammation. *Biomed Pharmacother*., **165**: 115085.

Zhong X and Chen R (2023). Detection of ferroptosis by immunohistochemistry and immunofluorescence. *Methods Mol Biol*., **2712**: 211–222.

Zhou GQ, Chen G, Yang J, Qin WY and Ping J (2022). Guizhi-Shaoyao-Zhimu decoction attenuates monosodium urate crystal-induced inflammation through inactivation of NF-κB and NLRP3 inflammasome. *J Ethnopharmacol*., **283**: 114707.